RSC Advances

PAPER

View Article Online
View Journal | View Issue

Cite this: *RSC Adv.*, 2017, **7**, 24833

Confinement of alcohols to enhance CO_2 capture in MIL-53(Al)†

Gerardo A. González-Martínez,‡[a] J. Antonio Zárate,‡[a] Ana Martínez,*[a] Elí Sánchez-González,[a] J. Raziel Álvarez,[a] Enrique Lima,[a] Eduardo González-Zamora*[b] and Ilich A. Ibarra*[a]

Received 28th March 2017
Accepted 2nd May 2017

DOI: 10.1039/c7ra03608f

rsc.li/rsc-advances

CO_2 capture of MIL-53(Al) was enhanced by confining MeOH and *i*-PrOH within its micropores. Compared to MIL-53(Al), results showed an approximately 1.3 fold increase in CO_2 capture capacity (kinetic isothermal CO_2 adsorption experiments), *via* confining small amounts of both alcohols. Adsorption–desorption properties are investigated for MeOH and *i*-PrOH and the enthalpy of adsorption, for MeOH and *i*-PrOH, was measured by differential scanning calorimetry (DSC): ΔH = 50 and 56 kJ mol^{-1}, respectively. Regeneration (CO_2 adsorption–desorption cycles) of the sample MeOH@MIL-53(Al) exhibited a loss on the CO_2 capacity of only 6.3% after 10 cycles and the desorption is accomplished by only turning the CO_2 flow off. Static CO_2 adsorption experiments (at 196 K) demonstrated a 1.25-fold CO_2 capture increase (from 7.2 mmol g^{-1}, fully activated MIL-53(Al) to 9.0 mmol g^{-1}, MeOH@MIL-53(Al)). The CO_2 enthalpy of adsorption for MIL-53(Al) and Me@OHMIL-53(Al) were estimated to be ΔH = 42.1 and 50.3 kJ mol^{-1}, respectively. Computational calculations demonstrated the role of the hydrogen bonds formed between CO_2 molecules and confined MeOH and *i*-PrOH molecules, resulting in the enhancement of the overall CO_2 capture.

Introduction

The physicochemical properties (*e.g.* dynamics and structure) in nanometre confining porous scales of condensed matter are considerably different to what is observed at the macroscopic level. Typically, gas solubility in solvents, including those confined in macroporous solid materials, is normally defined by Henry's Law, which postulates a linear relationship between the concentration of a dissolved gas and its partial pressure above the solvent.[1] Although, some recent investigations have shown that the confinement of solvents in porous materials, considerably enhances the gas solubility with respect to the values predicted by Henry's law. This striking improvement is known as "oversolubility".[2] The oversolubility of confined solvents considerably modifies their viscosity, density, dielectric constant and specific heat.[3] For example, Garcia-Garibay *et al.*[4] demonstrated in a MOF material (UCLA-R3) that the confinement of DMF molecules considerably enhanced (4 orders of magnitude) its dynamic viscosity which was comparable to that of honey.

Focusing on gas oversolubility (or gas enhancement by confining solvents), Luzar and Bratko[5] showed by computational simulations (molecular dynamics, MD) an increase of N_2 and O_2 solubility in water (from 5-fold to 10-fold) under confinement conditions in hydrophobic mesopores. By confining *n*-hexane, $CHCl_3$, EtOH and H_2O in mesostructured materials (MCM-41, SBA-15 and silica aerogel), remarkable H_2 solubility enhancements, were reported by Pera-Titus and co-workers.[1,6] Pellenq[7] confined *N*-methyl-2-pyrrolydone (NMP) in MCM-41 and demonstrated a 6-fold increase in CO_2 solubility. Interestingly, Llewellyn[8] reported a 5-fold increase in CO_2 capture by confining water in a mesoporous MOF material entitled MIL-100(Fe). This striking CO_2 increase was achieved when approximately 40 wt% of H_2O was pre-adsorbed in the mesopores of MIL-100(Fe).

In all the previous examples only mesoporous materials showed gas oversolubility properties. Interestingly, for microporous materials this phenomenon has not been observed as thoroughly demonstrated by Llewellyn and co-workers[8] in a MOF microporous material UiO-66. Thus, in order to referring to gas oversolubility it is necessary to incorporate (pre-adsorb) considerably high amounts of solvent (*e.g.* H_2O, *n*-hexane and EtOH) prior any gas adsorption. For example, Farrusseng *et al.*[9] remarkably reported a 22-fold improvement on the H_2 uptake (at 298 K and 30 bar) on MIL-101(Cr) by confining *n*-hexane. By a solvent wet impregnation method,[9] they loaded *n*-hexane into the fully activated MOF material and this corresponded to the

[a]*Laboratorio de Fisicoquímica y Reactividad de Superficies (LaFReS), Instituto de Investigaciones en Materiales, Universidad Nacional Autónoma de México, Circuito Exterior S/N, CU, Del. Coyoacán, 04510, Ciudad de México, Mexico. E-mail: argel@unam.mx; egz@xanum.uam.mx; martina@unam.mx; Fax: +52-55-5622-4595*

[b]*Departamento de Química, Universidad Autónoma Metropolitana-Iztapalapa, San Rafael Atlixco 186, Col. Vicentina, Iztapalapa, C. P. 09340, Ciudad de México, Mexico*

† Electronic supplementary information (ESI) available: TGA data, PXRD data, DSC data, activation protocol, isosteric enthalpy of adsorption data and theoretical calculations. See DOI: 10.1039/c7ra03608f

‡ These authors contributed equally to this work.

60% of the pore volume. In other words, 60% of the pore volume of MIL-101(Cr), was filled with *n*-hexane.

However, it is possible to confine small amounts of solvents in micropores materials to enhance gas adsorption properties. Certainly, this phenomenon cannot be referred as gas oversolubility since there is not "enough" solvent to solubilise gas molecules. Walton *et al.*[10] exhibited that small amounts of water can enhance CO_2 capture in microporous MOF materials. These small amounts of H_2O can interact with selected functional groups within the pores of these materials. In particular, they demonstrated that hydroxyl (–OH) functional groups act as a directing agent for water molecules inside the pores allowing a more efficient and ordered packing of H_2O.[11] In addition, Yaghi[12] showed that these functional groups (–OH), significantly improve the affinity of MOF materials to water.

Previously, we have demonstrated that small amounts of pre-adsorbed H_2O into microporous MOF materials considerably enhanced their CO_2 capture properties.[13] Additionally, our research group started to investigate the confinement of alcohols in MOFs to increase their CO_2 capture capabilities and this was exemplified with the pre-adsorption of small amounts of EtOH in InOF-1.[14] Therefore, we continue with the development of hybrid adsorbent MOF materials (*via* confining small amounts of alcohols within their micropores) which can contribute to new CO_2 capture technologies.[15] Among 'the twelve principles of CO_2 chemistry' that Poliakoff[16] proposed, CO_2 capture constitutes one of these challenges (maximise integration). Therefore, the search for post-synthetically modified MOFs with high structural stability, adsorption capacity, solvent stability, fast sorption kinetics and mild regeneration conditions, is nowadays a very hot research field.[17,18]

Herein, we report the augmented CO_2 capture properties of the microporous material MIL-53(Al), first reported by Serre and co-workers,[19] upon confining small amounts of alcohols (methanol and isopropanol), together with MeOH and *i*-PrOH adsorption–desorption properties of MIL-53(Al).

Experimental section

Synthetic preparations

MIL-53(Al), [Al(OH)(BDC)], was synthesised *via* a continuous flow process,[20] using merely water as the reaction medium. After the Al(III)-MOF material was synthesised, it went through a calcination process (extraction of terephthalic acid from within the pores of MIL-53(Al)) by heating the material up to 330 °C for 3 days. Thermogravimetric analysis (calcined MIL-53(Al)) (see Fig. S1, ESI†) and bulk powder X-ray diffraction patterns (see Fig. S2, ESI†) of the calcined MIL-53(Al) confirmed the retention of its structural integrity upon terephthalic acid removal. It is important to clarify, as previously reported,[19b,c] that the calcined MIL-53(Al), at room temperature, corresponds to the *lt* form (water molecules are located inside the channels of the material).[19b,c] When the calcined MOF sample is activated (180 °C and 10^{-3} bar for 2 h) there is a transformation from the *lt* form to the *ht* form.[19b,c] This characteristic structural transformation is very well known as the breathing effect of MIL-53.[19d] N_2 adsorption isotherms for activated MIL-53(Al), *vide supra*, at 77 K were used to estimate the BET surface area ($0.01 < P/P_0 < 0.04$) of 1098 $m^2\ g^{-1}$.

Adsorption isotherms for N_2, CO_2, MeOH and *i*-PrOH (isopropanol)

N_2 isotherms (up to 1 bar and 77 K) were recorded on a Belsorp mini II analyser under high vacuum in a clean system with a diaphragm pumping system. CO_2 isotherms up to 1 bar at 196 K, 212 K and 231 K, were recorded on a Belsorp HP (High Pressure) analyser. MeOH and *i*-PrOH isotherms were recorded in a DVS Advantage 1 instrument from Surface Measurement System. Ultra-pure grade (99.9995%) N_2 and CO_2 gases were purchased from PRAXAIR.

Kinetic CO_2 uptake experiments

Kinetic experiments were performed by using a thermobalance (Q500 HR, from TA) at 30 °C with a constant CO_2 flow (60 mL min^{-1}).

Results and discussion

Methanol and isopropanol adsorption studies

Methanol (MeOH) and isopropanol (*i*-PrOH) adsorption properties were investigated for MIL-53(Al). First, a sample of the calcined MIL-53(Al) was placed in an analyser cell (DVS Advantage 1 instrument) and activated at 180 °C for 2 h and under a flow of N_2. When the sample was fully degassed and cooled down to 30 °C, a methanol adsorption–desorption isotherm was carried out from $\%P/P_0 = 0$ to 85 (Fig. 1). The adsorbed amount of MeOH gradually increased with increasing pressure up to $\%P/P_0 = 10$. Then, a rapid MeOH uptake was observed in the pressure range from $\%P/P_0 = 10$ to 42. Finally, from $\%P/P_0 = 12$ to 85 there was a slow but gradual weight increase, and the maximum MeOH uptake was ~8.1 mmol g^{-1} (26.1 wt%). The overall MeOH isotherm exhibited a sigmoidal shape and a strong hysteresis loop (at $\%P/P_0 = 2$–12) was observed with marked stepped profiles in the desorption phase (Fig. 1, open circles). The pore dimensions of activated MIL-53(Al), *ht* form,[19b,c] are approximately 2.6 Å × 13.6 Å which are considerably much larger than the kinetic diameter of

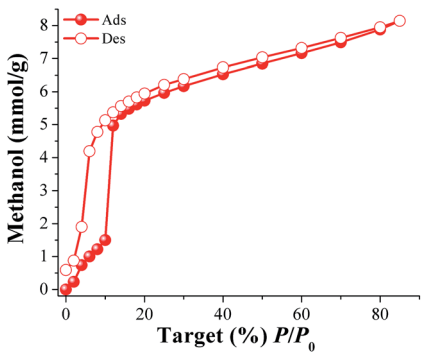

Fig. 1 Methanol adsorption isotherm at 30 °C of MIL-53(Al) from $\%P/P_0 = 0$ to 85. Solid circles represent adsorption, and open circles show desorption.

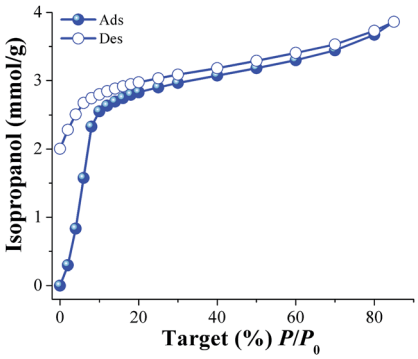

Fig. 2 Isopropanol adsorption isotherm at 30 °C of MIL-53(Al) from % P/P_0 = 0 to 85. Solid circles represent adsorption, and open circles show desorption.

methanol (~3.6 Å). Thus, the observed hysteresis is most likely due to moderately strong host–guest interactions, which result in an enhanced affinity of MIL-53(Al) for MeOH. These interactions are the result of methanol molecules forming hydrogen bonds with the bridging hydroxo functional groups (μ_2-OH), within the pores. This phenomenon was previously observed in a remarkable work by Maurin *et al.*[19e] They studied the methanol adsorption properties of MIL-53(Cr), an isostructural material to MIL-53(Al), finding a very similar MeOH adsorption–desorption isotherm and a strong and localised hydrogen bond between MeOH and the hydroxo functional group (μ_2-OH).[19e]

Later, a new calcined MIL-53(Al) sample was activated (as previously described) and an isopropanol adsorption–desorption isotherm was performed from $\%P/P_0$ = 0 to 85 at 30 °C (Fig. 2). To the best of our knowledge, this is the first time that the adsorption properties of isopropanol (*i*-PrOH) are described in MIL-53(Al). From 0 to 10 ($\%P/P_0$) the uptake of *i*-PrOH was rapidly increased (indicative of favourable host–guest interactions) achieving an *i*-PrOH uptake of approximately 2.5 mmol g^{-1} (15.3 wt%). Then, from $\%P/P_0$ = 10 to 85 a much slower (but constant) alcohol uptake was observed with a maximum of approximately 3.8 mmol g^{-1} (23.2 wt%). A relatively strong hysteresis was observed in the desorption phase (Fig. 2, open symbols). This hysteresis occurred mainly in the low pressure range from $\%P/P_0$ = 0 to 10. As in the previous case (MeOH), the kinetic diameter of *i*-PrOH is 4.6 Å which is considerably smaller than the pore openings of activated MIL-53(Al), (2.6 Å × 13.6 Å, *ht* form),[19b,c] suggesting again, the formation of hydrogen bonds with the bridging hydroxo functional groups (μ_2-OH).[19e]

When both alcohols (MeOH and *i*-PrOH) uptakes in MIL-53(Al) are compared at low loadings ($\%P/P_0$ = 0 to 10), there is a clear preference for *i*-PrOH over MeOH (2.5 *vs.* 1.4 mmol g^{-1}, respectively) which can be attributed to a stronger interaction of *i*-PrOH with the material. In order to confirm this, the enthalpy of adsorption (ΔH) for *i*-PrOH was experimentally measured by differential scanning calorimetry (DSC) from room temperature to 600 °C (with a ramp of 5 °C min^{-1}). The ΔH value was equal to 56 kJ mol^{-1} (see Fig. S3 ESI†). When the same experimental determination was performed for MeOH, the ΔH value was equal to 50 kJ mol^{-1} (see Fig. S4 ESI†), in good correlation with the alcohol uptakes (low loadings). When the total uptake of these alcohols is compared (MeOH = 8.1 mmol g^{-1} and *i*-PrOH = 3.8 mmol g^{-1}), MIL-53(Al) can adsorb considerably more MeOH than *i*-PrOH, presumably, due to the size of the alcohol molecules (methanol is smaller than isopropanol; kinetic diameters = 3.6 Å and 4.6 Å, respectively).

CO_2 capture studies

Isothermal and dynamic CO_2 adsorption experiments (kinetic) were performed on desolvated MIL-53(Al). First, a sample of the calcined MIL-53(Al) was placed inside a thermobalance (Q500 HR) and activated by heating from room temperature to 180 °C for 2 h and under a flow of pure N_2 gas flow. Then, the sample was cooled down to 30 °C under N_2 flow. After the sample had reached 30 °C, the N_2 purge flow was switched to 60 mL min^{-1} of CO_2. Fig. 3 (MIL-53(Al)) exhibits the kinetic CO_2 uptake experiment at 30 °C. At this temperature, the material showed the maximum weight percentage gain, which indicates the maximum amount of CO_2 captured. This amount corresponds to 3.5 wt%, which was rapidly reached after only 4 min remains constant until the end of the experiment (12 min), Fig. 3 (MIL-53(Al)).

Later, a calcined sample of MIL-53(Al) was activated (180 °C for 2 h and under a flow of N_2), cooled down to 30 °C (under N_2) and saturated with MeOH (see ESI†). After an activation protocol (see ESI†) the residual amount of MeOH was equal to 2 wt%. The reproducibility of this protocol was confirmed by performing 5 independent experiment (see ESI†). Hereinafter, this sample will be referred as MeOH@MIL-53(Al), $[Al(OH)(BDC)]\cdot MeOH_{0.08}$. Similar procedure was carried out for sample *i*-PrOH@MIL-53(Al), $[Al(OH)(BDC)]\cdot iPrOH_{0.05}$, as it is described in the ESI.†

It was decided to only pre-adsorbed small amounts of alcohols (MeOH and *i*-PrOH) in MIL-53(Al) samples, based on the investigation of confined H_2O in the micropores of MIL-53(Cr),[21] (a MOF material which is isostructural to MIL-53(Al)). Then, Paesani and co-workers[21] demonstrated by computational infrared spectroscopy that at low water loadings, these water molecules interact strongly with the hydroxo (μ_2-OH)

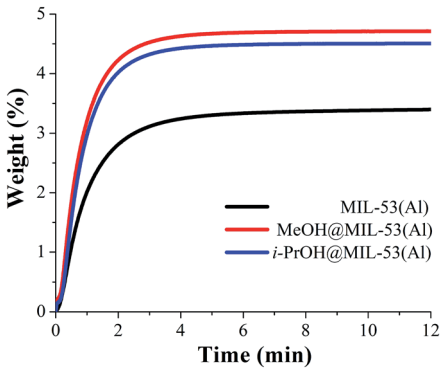

Fig. 3 Kinetic CO_2 uptake experiments performed at 30 °C with a CO_2 flow of 60 mL min^{-1} in MIL-53(Al), (black curve); MeOH@MIL-53(Al), (red curve) and *i*-PrOH@MIL-53(Al), (blue curve).

functional groups, *via* hydrogen bonding, which are located inside the pore walls of MIL-53(Cr). Continuing with the investigation of MIL-53, by different calculation methodologies, Haigis[22] employed molecular dynamics (MD), to show that H_2O molecules can form strong hydrogen bonds with the μ_2-OH functional groups, in MIL-53(Cr), as a function of water loading. In addition, Maurin *et al.*[23] corroborated by GCMC computational simulations, in MIL-53(Cr), that at low water loadings, these H_2O molecules are regularly accommodated inside all the pores of the material.

Certainly, all the previous computational approaches indicated the role of the μ_2-OH functional groups (inside the micropores of MIL-53(Cr)) to "pin" small amounts of water *via* hydrogen bonding. Complementing to these calculations, we experimentally demonstrated that small amounts of EtOH (2.6 wt%), confined within the micropores of InOF-1 (ref. 14) can: (i) hydrogen-bond to the similar hydroxo functional ($In_2(\mu_2$-OH)) which was visualised by single crystal X-ray diffraction; and (ii) significantly enhance CO_2 capture (2.7 fold).

Therefore, we rationalised the hypothesis of low MeOH and *i*-PrOH loadings where the micro-porous channels of MIL-53(Al) could efficiently accommodate these alcohols molecules. As a result of this very well ordered positioning of MeOH and *i*-PrOH, these confined alcohol molecules could help to pack more efficiently CO_2 molecules and finally enhance the total CO_2 capture.

Then, a kinetic CO_2 experiment, at 30 °C, was carried out on the MeOH@MIL-53(Al) sample. The maximum amount of CO_2 captured corresponded to 4.7 wt%, which was reached at approximately 4 min and it was constant until the end of the experiment (12 min), Fig. 3 (MeOH@MIL-53). It is important to mention that samples of MeOH@MIL-53(Al) were prepared with anhydrous methanol (<0.005% water) and methanol (reagent alcohol, 95%). The kinetic CO_2 experiments showed no difference in the maximum amount of CO_2 captured. Additionally, we also tried different small residual-amounts of MeOH: 3%, 4% and 5% and the best result was obtained with 2 wt% of MeOH.

Therefore, the CO_2 capture was approximately 1.3-fold improved (from 3.5 wt% to 4.7 wt%), when small amounts of MeOH were pre-adsorbed in MIL-53(Al). Moreover, the 1.3-fold increase was reached at the same time (~4 min) than the MIL-53(Al) sample, showing that the CO_2 adsorption kinetics were highly improved due to the MeOH presence.

Later, the sample *i*-PrOH@MIL-53(Al) was prepared as previously described (*vide supra* and see ESI†) where the amount of pre-adsorbed isopropanol was equal to 2 wt%. Fig. 3 exhibits the kinetic CO_2 experiment performed on *i*-PrOH@MIL-53(Al) and the maximum amount of adsorbed CO_2 (captured) was equal to 4.5 wt%. This value is slightly smaller to the one observed for sample MeOH@MIL-53(Al), indicating that the pre-adsorption of MeOH in MIL-53(Al) favours the overall capture of CO_2. It is worth to emphasise that the confinement of small amounts of both alcohols (2 wt%) enhances the CO_2 capture properties of this MOF material.

Long-term regeneration capacity is a fundamental parameter for any CO_2 capture material and it is desirable to show very low energy requirements for CO_2 release.[24] In industrial separation processes this step is typically very expensive and complicated.[25] Among many current methodologies to this target, perhaps, the most common is the use of vacuum and temperature swing adsorption. For example, Long and co-workers[26] reported a working CO_2 capacity (total CO_2 adsorption) of ~7 wt% at room temperature (25 °C) on mmen-CuBTTri. This MOF material was regenerated by switching the flow (15% CO_2 in N_2) to a pure N_2 stream followed by increasing the temperature up to 60 °C. Denayer and co-workers[27] reported a total CO_2 adsorption of 3.7 wt% for NH_2-MIL-53 and the regeneration of this material was performed under purge flow at 159 °C.

In order to evaluate the regeneration properties of MeOH@MIL-53(Al), a new sample was prepared (by confining 2 wt% of MeOH in MIL-53(Al)) and kinetic CO_2 adsorption–desorption experiments, at 30 °C, were carried on (Fig. 4). We decided to only evaluate the regeneration properties of MeOH@MIL-53(Al) since it showed the best CO_2 capture result. Each cycle consists of an adsorption step (15 min) and a desorption step (15 min), providing a cycling time of only 30 min without the use of N_2 purge nor increasing the temperature.

Simply, by turning off the CO_2 flow (corresponding to the desorption step) and keeping the adsorption temperature (30 °C), the total regeneration of the MeOH@MIL-53(Al) sample was accomplished. Form the first cycle (4.7 wt% CO_2 adsorption) to the tenth cycle (4.4 wt% CO_2 adsorption) it was observed a loss of the CO_2 capacity (from 4.7 to 4.4 wt%) which represents a loss on the CO_2 capacity of only 6.3% (Fig. 4). Although there was a small loss in the CO_2 capacity, this result is noteworthy since there is no need to use a purge gas (*e.g.* N_2) and more significantly no thermal re-activation of the sample is required, resulting in a very low cost separation process.

In order to describe the CO_2 adsorption properties of MeOH@MIL-53(Al), we performed static (increasing the partial pressure from 0 to 1 bar) and isothermal (196 K) CO_2 adsorption experiments on MeOH@MIL-53(Al) samples. It was decided to perform these experiments at 196 K since the adsorption of CO_2 at 30 °C (303 K) is problematic due to proximity to the critical temperature of CO_2.[28] The uncertainly of the δ_{CO_2} (density) of the CO_2 adsorbed, and since at that temperature the CO_2 saturation

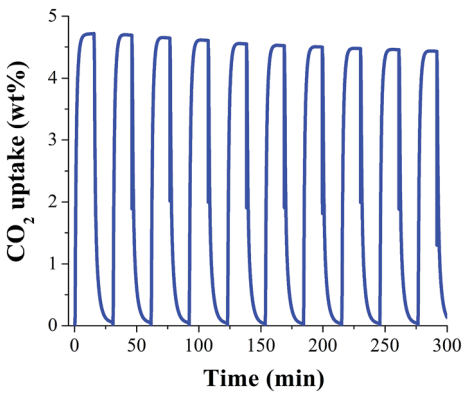

Fig. 4 Adsorption–desorption cycling for MeOH@MIL-53(Al), showing a reversible CO_2.

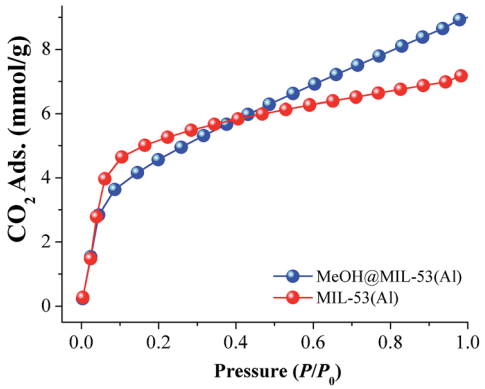

Fig. 5 Static CO_2 adsorption performed from 0 to 1 bar at 196 K on MIL-53(Al), (red circles) and MeOH@MIL-53(Al), (blue circles).

pressure is extremely high, the range of P/P_0 is limited to 0.02 at sub-atmospheric pressures.[29] It has been proposed that adsorption in well-defined micropores occurs by a pore-filling mechanism rather than surface coverage.[29,30] As an example, N_2 molecules at 77 K can fill these micropores in a liquid-like fashion at very low relative pressures (below 0.01). On the other hand, CO_2 adsorbed at approximately ambient temperatures (298 or 303 K) can only form a monolayer on the walls of the micropores.[30] Therefore, to accomplish pore-filling within the micropores of MOFs and a more accurate description of the CO_2 adsorption properties of these microporous materials, CO_2 gas adsorption experiments at 196 K are preferred.[31]

First, a CO_2 adsorption experiment at 196 K was carried on a fully activated (180 °C for 1 h and 10^{-3} bar) sample of MIL-53(Al) exhibiting a total CO_2 uptake of 7.2 mmol g^{-1} (31.7 wt%), (see Fig. 5, MIL-53(Al)). Later, a MeOH@MIL-53(Al) sample was placed in a high-pressure cell (Belsorp HP) and gently evacuated to remove any absorbed moisture. The CO_2 uptake was measured from 0 to 1 bar at 196 K and the resultant CO_2 adsorption exhibited a characteristic Type-I isotherm with a total CO_2 capture of 9.0 mmol g^{-1} (39.6 wt%), (Fig. 5, MeOH@MIL-53(Al)). Then, at 1 bar and 196 K, the CO_2 capture was approximately 1.25-fold increased (from 7.2 to 9.0 mmol g^{-1}) when small amounts of MeOH are present within the micropores of MIL-53(Al). The evaluation of the BET surface area of MeOH@MIL-53(Al) was equal to 762 m^2 g^{-1} with a pore volume of 0.39 cm^3 g^{-1} (lower values than for the fully activated MIL-53(Al), BET = 1096 m^2 g^{-1} and pore volume = 0.56 cm^3 g^{-1}). In addition, we measured CO_2 adsorption isotherms at 212 K (dry ice and chloroform bath) and 231 K (dry ice and acetonitrile bath), in order to calculate the enthalpy of adsorption (ΔH) by isosteric method for both samples: MIL-53(Al) and MeOH@MIL-53(Al), (see Fig. S5–S8 ESI†). The values were estimated to be 42.1 and 50.3 kJ mol^{-1} for MIL-53(Al) and MeOH@MIL-53(Al), respectively. Thus, ΔH for CO_2 was enhanced when small quantities of MeOH are confined within the material MIL-53(Al).

Computational studies

In order to investigate the relationship between the presence of methanol and isopropanol (confined into MIL-53(Al)) and their

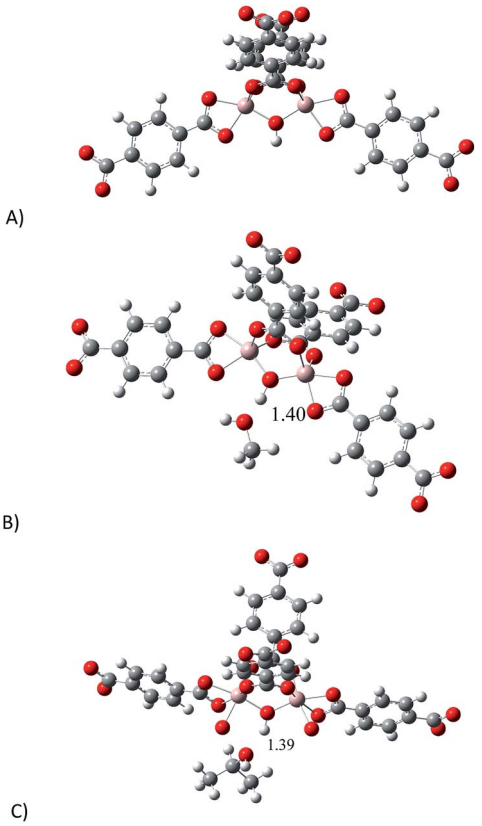

Fig. 6 Optimised structures of: (A) proposed model to represent the active site; (B) model interacting with MeOH and (C) model interacting with *i*-PrOH.

affinity towards CO_2, a model of the binuclear [$Al_2(\mu_2$-OH)] building block (reactive section) was taken and the geometry was optimised (see ESI,† computational details). Since the most representative section of the model is related to the μ_2-OH group, we decided to study the interactions between μ_2-OH and the incorporation of different analytes (MeOH, *i*-PrOH and CO_2). Fig. 6 shows the optimised structure of the proposed model (A) and the optimised structures for the model interacting with MeOH (B) and *i*-PrOH (C). As it was expected, both alcohols form hydrogen bonds with the μ_2-OH group. Bond distances of these hydrogen bonds are very similar (1.39 and 1.40 Å). Our computations suggest that the interaction of both alcohol molecules (MeOH and *i*-PrOH) with the μ_2-OH group of the model is very similar, since the distance of the hydrogen bond is practically the same. This result correlates with the small CO_2 capture difference on confining small amounts of MeOH *vs.* *i*-PrOH within MIL-53(Al), see Fig. 3.

Later, we introduced a single CO_2 molecule in all the optimised structures: proposed model (empty) and the models interacting with MeOH and *i*-PrOH. In Fig. 7 is presented the optimised structures of all the models interacting with CO_2. As expected, the single CO_2 molecule forms hydrogen bonds in all the structures. It is very well studied that the hydrogen bond distance is an indication on the strength of the interaction between molecules.[32] Thus, If we compare the μ_2-OH···O=C=O bond distances, it is possible to observe that the structure

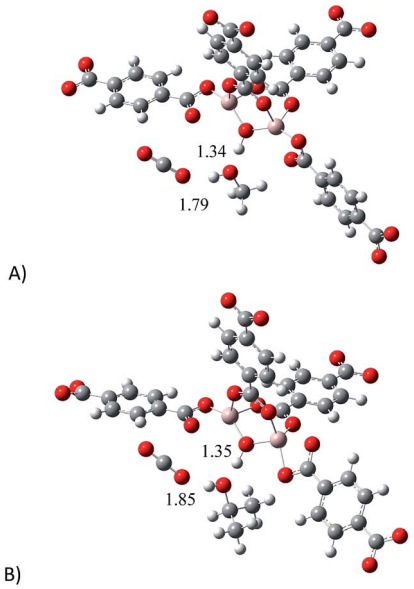

Fig. 7 Optimised structures of: (A) proposed model interacting with MeOH and CO_2 and (B) proposed model interacting with *i*-PrOH and CO_2.

containing MeOH establishes a shorter hydrogen bond (1.79 Å, Fig. 7A) than the structure with *i*-PrOH (1.85 Å, Fig. 7B). This slight difference, in the bond length, can actually explain the small dissimilarity in the overall capture of CO_2 when small amounts of the alcohols are confined within the MOF material MIL-53(Al), see Fig. 3. Therefore, our computational calculations highlighted the significance of the hydrogen bonds formed between CO_2 molecules and confined alcohol molecules: on increasing the strength (diminishing the distance) of the hydrogen bond between the μ_2-OH group and the confined alcohol, the overall ability to capture CO_2 increases.

Conclusions

The microporous Al(III)-based MOF material MIL-53(Al) exhibited, by kinetic isotherm CO_2 experiments, a total CO_2 uptake of 3.5 wt%. When confining small amounts of methanol (MeOH) and isopropanol (*i*-PrOH) (2 wt%) within MIL-53(Al), the CO_2 capture incremented to 4.7 and 4.5 wt%, respectively, which approximately corresponds to a 1.3-fold increase. MeOH and *i*-PrOH adsorption properties were investigated for MIL-53(Al). Uptakes (at low loadings: $\%P/P_0 = 0$ to 10) of both alcohols in MIL-53(Al) showed a clear preference for *i*-PrOH over MeOH (2.5 *vs.* 1.4 mmol g^{-1}, respectively) which was attributed to a stronger interaction of *i*-PrOH with the material. Enthalpy of adsorption (ΔH) for *i*-PrOH and MeOH were experimentally measured by differential scanning calorimetry (DSC) with values of $\Delta H = 56$ and 50 kJ mol^{-1}, respectively. MeOH@MIL-53(Al) can reversibly adsorb/desorb CO_2 with a loss on the CO_2 capacity of only 6.3% after 10 cycles and the desorption is performed by turning the CO_2 flow off without the need to change the temperature or use inert gas. Static and isothermal CO_2 experiments (from 0 to 1 bar of CO_2 at 196 K) also demonstrated a 1.25-fold CO_2 capture increase (from 7.2 mmol g^{-1}, MIL-53(Al) fully activated to 9.0 mmol g^{-1}, MeOH@MIL-53(Al)). The CO_2 enthalpy of adsorption for MIL-53(Al) and MeOHMIL-53(Al) were calculated from CO_2 adsorption isotherms at 212 K and 231 K to be $\Delta H =$ 42.1 and 50.3 kJ mol^{-1}, respectively. Quantum calculations demonstrated the role of the hydrogen bonds formed between CO_2 molecules and confined MeOH and *i*-PrOH molecules: on increasing the strength (shorting the distance) of the hydrogen bond between the hydroxo functional group (μ_2-OH) group and the confined alcohol, the overall result is the enhancement of the CO_2 capture. We are currently exploring other MOF materials and the confinement of different solvents (polar and non-polar) which could enhance CO_2 capture in MOFs.

Acknowledgements

The authors thank Dr A. Tejeda-Cruz (X-ray; IIM-UNAM), CONACyT Mexico (212318), PAPIIT UNAM Mexico (IN100415) for financial support. E. G.-Z. thanks CONACyT (236879), Mexico for financial support. Thanks to U. Winnberg (ITAM) for scientific discussions. Thanks to Eriseth R.-Morales for acces to Laboratorio de Análisis Térmico. NES supercomputer, provided by DGTIC-UNAM. Oralia L Jiménez, María Teresa Vázquez and Caín González for their technical support.

Notes and references

1 S. Miachon, V. V. Syakaev, A. Rakhmatullin, M. Pera-Titus, S. Caldarelli and J.-A. Dalmon, *ChemPhysChem*, 2008, **9**, 78.
2 (*a*) S. Clauzier, L. N. Ho, M. Pera-Titus, D. Farrusseng and B. Coasne, *J. Phys. Chem. C*, 2014, **118**, 10720; (*b*) L. N. Ho, Y. Schuurman, D. Farrusseng and B. Coasne, *J. Phys. Chem. C*, 2015, **119**, 21547.
3 (*a*) F. Volino, H. Gérard and S. Miachon, *Ann. Phys.*, 1997, **22**, 43; (*b*) K. Morishige and M. Shikimi, *J. Chem. Phys.*, 1998, **108**, 7821; (*c*) M. O. Kimball and F. M. Gasparini, *Phys. Rev. Lett.*, 2005, **95**, 165701; (*d*) U. Zammit, M. Marinelli, F. Mercuri and S. Paoloni, *J. Phys. Chem. B*, 2009, **113**, 14315.
4 X. Jiang, H.-B. Duan, S. I. Khan and M. A. Garcia-Garibay, *ACS Cent. Sci.*, 2016, **2**, 608.
5 (*a*) A. Luzar and D. Bratko, *J. Phys. Chem. B*, 2005, **109**, 22545; (*b*) D. Bratko and A. Luzar, *Langmuir*, 2008, **24**, 1247.
6 (*a*) M. Pera-Titus, R. El-Chahal, V. Rakotovao, S. Miachon and J.-A. Dalmon, *ChemPhysChem*, 2009, **10**, 2082; (*b*) M. Pera-Titus, S. Miachon and J.-A. Dalmon, *AIChE J.*, 2009, **55**, 434; (*c*) V. Rakotovao, R. Ammar, S. Miachon and M. Pera-Titus, *Chem. Phys. Lett.*, 2010, **485**, 299.
7 (*a*) N. L. Ho, J. Perez-Pellitero, F. Porcheron and R. J.-M. Pellenq, *J. Phys. Chem. C*, 2012, **116**, 3600; (*b*) N. L. Ho, J. Perez-Pellitero, F. Porcheron and R. J.-M. Pellenq, *Langmuir*, 2011, **27**, 8187; (*c*) N. L. Ho, F. Porcheron and R. J.-M. Pellenq, *Langmuir*, 2010, **26**, 13287.
8 E. Soubeyrand-Lenoir, C. Vagner, J. W. Yoon, P. Bazin, F. Ragon, Y. K. Hwang, C. Serre, J.-S. Chang and P. L. Llewellyn, *J. Am. Chem. Soc.*, 2012, **134**, 10174.
9 S. Clauzier, L. N. Ho, M. Pera-Titus, B. Coasne and D. Farrusseng, *J. Am. Chem. Soc.*, 2012, **134**, 17369.

10 (*a*) H. Jasuja, Y.-G. Huang and K. S. Walton, *Langmuir*, 2012, **28**, 16874; (*b*) H. Jasuja, J. Zang, D. S. Sholl and K. S. Walton, *J. Phys. Chem. C*, 2012, **116**, 23526; (*c*) J. B. DeCoste, G. W. Peterson, H. Jasuja, T. G. Glover, Y.-G. Huang and K. S. Walton, *J. Mater. Chem. A*, 2013, **1**, 5642; (*d*) N. C. Burtch, H. Jasuja and K. S. Walton, *Chem. Rev.*, 2014, **114**, 10575.

11 G. E. Cmarik, M. Kim, S. M. Cohen and K. S. Walton, *Langmuir*, 2012, **28**, 15606.

12 H. Furukawa, F. Gándara, Y.-B. Zhang, J. Jiang, W. L. Queen, M. R. Hudson and O. M. Yahgi, *J. Am. Chem. Soc.*, 2014, **136**, 4369.

13 (*a*) M. R. Gonzalez, J. H. González-Estefan, H. A. Lara-García, P. Sánchez-Camacho, E. I. Basaldella, H. Pfeiffer and I. A. Ibarra, *New J. Chem.*, 2015, **39**, 2400; (*b*) H. A. Lara-García, M. R. Gonzalez, J. H. González-Estefan, P. Sánchez-Camacho, E. Lima and I. A. Ibarra, *Inorg. Chem. Front.*, 2015, **2**, 442; (*c*) R. A. Peralta, B. Alcántar-Vázquez, M. Sánchez-Serratos, E. González-Zamora and I. A. Ibarra, *Inorg. Chem. Front.*, 2015, **2**, 898; (*d*) J. R. Álvarez, R. A. Peralta, J. Balmaseda, E. González-Zamora and I. A. Ibarra, *Inorg. Chem. Front.*, 2015, **2**, 1080; (*e*) M. Sánchez-Serratos, P. A. Bayliss, R. A. Peralta, E. González-Zamora, E. Lima and I. A. Ibarra, *New J. Chem.*, 2016, **40**, 68; (*f*) A. Zárate, R. A. Peralta, P. A. Bayliss, R. Howie, M. Sánchez-Serratos, P. Carmona-Monroy, D. Solis-Ibarra, E. González-Zamora and I. A. Ibarra, *RSC Adv.*, 2016, **6**, 9978; (*g*) E. Sánchez-González, J. R. Álvarez, R. A. Peralta, A. Campos-Reales-Pineda, A. Tejeda-Cruz, E. Lima, J. Balmaseda, E. González-Zamora and I. A. Ibarra, *ACS Omega*, 2016, **1**, 305; (*h*) E. González-Zamora and I. A. Ibarra, *Mater. Chem. Front.*, 2017, DOI: 10.1039/C6QM00301J.

14 R. A. Peralta, A. Campos-Reales-Pineda, H. Pfeiffer, J. R. Álvarez, J. A. Zárate, J. Balmaseda, E. González-Zamora, A. Martínez, D. Martínez-Otero, V. Jancik and I. A. Ibarra, *Chem. Commun.*, 2016, **52**, 10273.

15 (*a*) D. M. D'Alessandro, B. Smit and J. R. Long, *Angew. Chem., Int. Ed.*, 2010, **49**, 6058; (*b*) K. Sumida, D. L. Rogow, J. A. Mason, T. M. McDonald, E. D. Bloch, Z. R. Herm, Z. T.-H. Bae and J. R. Long, *Chem. Rev.*, 2012, **112**, 724.

16 M. Poliakoff, W. Leitner and E. S. Streng, *Faraday Discuss.*, 2015, **183**, 9.

17 (*a*) S. Yang, G. S. B. Martin, J. J. Titman, A. J. Blake, D. R. Allan, N. R. Champness and M. Schröder, *Inorg. Chem.*, 2011, **50**, 9374; (*b*) S. Yang, X. Lin, A. J. Blake, G. S. Walker, P. Hubberstey, N. R. Champness and M. Schröder, *Nat. Chem.*, 2009, **1**, 487; (*c*) A. J. Nuñez, L. N. Shear, N. Dahal, I. A. Ibarra, J. W. Yoon, Y. K. Hwang, J.-S. Chang and S. M. Humphrey, *Chem. Commun.*, 2011, **47**, 11855; (*d*) I. A. Ibarra, J. W. Yoon, J.-S. Chang, S. K. Lee, V. M. Lynch and S. M. Humphrey, *Inorg. Chem.*, 2012, **51**, 12242; (*e*) X. Lin, A. J. Blake, C. Wilson, X. Z. Sun, N. R. Champness, M. W. George, P. Hubberstey, R. Mokaya and M. Schröder, *J. Am. Chem. Soc.*, 2006, **128**, 10745; (*f*) P. Nugent, Y. Belmabkhout, S. D. Burd, A. J. Cairns, R. Luebke, K. Forrest, T. Pham, S. Ma, B. Space, L. Wojtas, M. Eddaoudi and M. J. Zaworotko, *Nature*, 2013, **495**, 80; (*g*) O. Shekhah, Y. Belmabkhout, Z. Chen, V. Guillerm, A. Cairns, K. Adil and M. Eddaoudi, *Nat. Commun.*, 2014, **5**, 522; (*h*) W. M. Bloch, A. Burgun, C. J. Coghlan, R. Lee, M. L. Coote, C. J. Doonan and C. J. Sumby, *Nat. Chem.*, 2014, **6**, 906; (*i*) K. Okada, R. Ricco, Y. Tokudome, M. J. Styles, A. J. Hill, M. Takahashi and P. Falcaro, *Adv. Funct. Mater.*, 2014, **24**, 1969; (*j*) H. Li, M. R. Hill, R. Huang, C. Doblin, S. Lim, A. J. Hill, R. Babarao and P. Falcaro, *Chem. Commun.*, 2016, **52**, 5973; (*k*) K. Sumida, N. Moitra, J. Reboul, S. Fukumoto, K. Nakanishi, K. Kanamori, S. Furukawa and S. Kitagawa, *Chem. Sci.*, 2015, **6**, 5938; (*l*) K. Hirai, S. Furukawa, M. Kondo, H. Uehara, O. Sakata and S. Kitagawa, *Angew. Chem., Int. Ed.*, 2011, **50**, 8057.

18 (*a*) T. Tozawa, J. T. A. Jones, S. I. Swamy, S. Jiang, D. J. Adams, S. Shakespeare, R. Clowes, D. Bradshaw, T. Hasell, S. Y. Chong, C. Tang, S. Thompson, J. Parker, A. Trewin, J. Bacsa, A. M. Z. Slawin, A. Steiner and A. I. Cooper, *Nat. Mater.*, 2009, **8**, 973; (*b*) R. Dawson, D. J. Adams and A. I. Cooper, *Chem. Sci.*, 2011, **2**, 1173; (*c*) W. M. Bloch, R. Babarao, M. R. Hill, C. J. Doonan and C. J. Sumby, *J. Am. Chem. Soc.*, 2013, **135**, 10441; (*d*) J. A. Mason, K. Sumida, Z. R. Herm, R. Krishna and J. R. Long, *Energy Environ. Sci.*, 2011, **4**, 3030; (*e*) R. Babarao, C. J. Coghlan, D. Rankine, W. M. Bloch, G. K. Gransbury, H. Sato, S. Kitagawa, C. J. Sumby, M. R. Hill and C. J. Doonan, *Chem. Commun.*, 2014, **50**, 3238; (*f*) I. A. Ibarra, A. Mace, S. Yang, J. Sun, S. Lee, J.-S. Chang, A. Laaksonen, M. Schröder and X. Zou, *Inorg. Chem.*, 2016, **55**, 7219; (*g*) A. López-Olvera, E. Sánchez-González, A. Campos-Reales-Pineda, A. Aguilar-Granda, I. A. Ibarra and B. Rodríguez-Molina, *Inorg. Chem. Front.*, 2017, **4**, 56.

19 (*a*) G. Férey, M. Latroche, C. Serre, F. Millange, T. Loiseau and A. Percheron-Guégan, *Chem. Commun.*, 2003, 2976; (*b*) T. Loiseau, C. Serre, C. Huguenard, G. Fink, F. Taulell, M. Henry, T. Bataille and G. Férey, *Chem.–Eur. J.*, 2004, **10**, 1373; (*c*) P. L. Llewellyn, G. Maurin, T. Devic, S. Loera-Serna, N. Rosenbach, C. Serre, S. Bourrelly, P. Horcajada, Y. Filinchuk and G. Férey, *J. Am. Chem. Soc.*, 2010, **132**, 9488; (*d*) G. Férey and C. Serre, *Chem. Soc. Rev.*, 2009, **38**, 1380; (*e*) S. Bourrelly, B. Moulin, A. Rivera, G. Maurin, S. Devautour-Vinot, C. Serre, T. Devic, P. Horcajada, A. Vimont, G. Clet, M. Daturi, J.-C. Lavalley, S. Loera-Serna, R. Denoyel, P. L. Llewellyn and G. Férey, *J. Am. Chem. Soc.*, 2010, **132**, 9488.

20 P. A. Bayliss, I. A. Ibarra, E. Pérez, S. Yang, C. C. Tang, M. Poliakoff and M. Schörder, *Green Chem.*, 2014, **16**, 3796.

21 G. R. Medders and F. Paesani, *J. Phys. Chem. Lett.*, 2014, **5**, 2897.

22 V. Haigis, F.-X. Coudert, R. Vuilleumier and A. Boutin, *Phys. Chem. Chem. Phys.*, 2013, **15**, 19049.

23 F. Salles, S. Bourrelly, H. Jobic, T. Devic, V. Guillerm, P. Llewellyn, C. Serre, G. Férey and G. Maurin, *J. Phys. Chem. C*, 2011, **115**, 10764.

24 R. A. Khatri, S. S. C. Chuang, Y. Soong and M. Gray, *Ind. Eng. Chem. Res.*, 2005, **44**, 3702.

25 B. Metz, O. Davidson, H. de Coninck, M. Loos and L. Meyer, *IPCC Special Report: Carbon Dioxide Capture and Storage*, 2005.
26 T. M. Mcdonald, D. M. D'Alessandro, R. Krishna and J. R. Long, *Chem. Sci.*, 2011, **2**, 2022.
27 S. Couck, J. F. M. Denayer, G. V. Baron, T. Rémy, J. Gascon and F. Kapteijn, *J. Am. Chem. Soc.*, 2009, **131**, 6326.
28 D. R. Lide, *Handbook of Chemistry and Physics*, CRC Press LLC, 2004.
29 F. Rouquerol, J. Rouquerol, K. S. W. Sing, P. Llewellyn and G. Maurin, *Adsorption by Powders and Porous Solids; Principles, Methodology and Applications*, Elsevier Press, 2014.
30 J. Garrido, A. Linares-Solano, J. M. Martín-Martínez, M. Molina-Sabio, F. Rodríguez-Reinoso and R. Torregrosa, *Langmuir*, 1987, **3**, 76.
31 (*a*) H. J. Park and M. P. Sun, *Chem.–Eur. J.*, 2008, **14**, 8812; (*b*) I. A. Ibarra, K. E. Tan, V. M. Lynch and S. M. Humphrey, *Dalton Trans.*, 2012, **41**, 3920; (*c*) S. M. Humphrey, J.-S. Chang, S. H. Jhung, J. W. Yoon and P. T. Wood, *Angew. Chem., Int. Ed*, 2007, **46**, 272; (*d*) J. Lee, N. W. Waggoner, L. Polanco, G. R. You, V. M. Lynch, S. K. Kim, S. M. Humphrey and J. L. Sessler, *Chem. Commun.*, 2016, **52**, 8514.
32 R. Vargas, J. Garza, D. A. Dixon and B. Hay, *J. Am. Chem. Soc.*, 2000, **122**, 4750.